Proc. Natl. Acad. Sci. USA
Vol. 81, pp. 4950–4954, August 1984
Medical Sciences

In vivo, cAMP stimulates growth and morphogenesis of mouse mammary ducts

(mammary epithelium/cholera toxin/ductal development)

GARY B. SILBERSTEIN, PHYLLIS STRICKLAND, VIRGINIA TRUMPBOUR, SUSANNE COLEMAN, AND CHARLES W. DANIEL

Department of Biology, Thimann Laboratories, University of California, Santa Cruz, CA 95064

Communicated by Kenneth V. Thimann, April 16, 1984

ABSTRACT **In culture, cAMP is known to be mitogenic for mammary cells and several other epithelia, but evidence for a similar role *in vivo* has been only correlative. We have used plastic implants to cause slow release of cholera toxin and other cAMP-active agents to local areas of mammary glands in ovariectomized mice. Elevated levels of intracellular cAMP around the implants promoted vigorous growth and normal ductal morphogenesis, while distant sites were unaffected. Local effects of cAMP included restoration of normal ductal caliber, formation of new end buds, and reinitiation of DNA synthesis in both epithelium and surrounding stroma. Thus, cAMP is both a mitogenic and a morphogenetic factor in this tissue.**

Numerous *in vitro* studies have shown cAMP to be growth promoting for mouse, rat, and human mammary epithelia (1–4) and for a variety of other epithelial cell types (5–8). *In situ*, cAMP levels increase as the mammary gland grows during pregnancy (9, 10), and they are elevated in several breast carcinomas (11, 12). To obtain more direct evidence as to whether cAMP may function as an intracellular mediator of hormone or growth factor action in the mammary gland, we investigated the effects of raising cAMP levels in small regions of the mouse mammary gland by using slow-release plastic implants.

End buds, the primary sites of mammary epithelial proliferation in subadult virgin mice, are complex highly mitotic structures comprised of the stem cell progenitors of myoepithelial and ductal cells (13). As the growth points for the ductal tree, end buds are the focus of mammary growth regulatory influences during this stage in development of the gland (14). We here present evidence that, *in situ*, local elevation of cAMP stimulated formation of new end buds in regressed ducts, apparently replacing the normal hormonal requirements for this type of development.

MATERIALS AND METHODS

Materials. Ethylene/vinyl acetate copolymer (Elvax, 40% vinyl acetate by weight) was a gift of DuPont. Alcian blue 8GX was from MCB Manufacturing Chemists (Cincinnati, OH). Complete cholera toxin (CT), CT subunits A and B (CT-A and CT-B), isoproterenol, cAMP, dibutyryl cAMP, 8-bromo cAMP, butyrate, and theophylline were from Sigma. Forskolin was from Calbiochem. Tritiated thymidine (79.2 Ci/mmol; 1 Ci = 37 GBq) was from New England Nuclear. Anti-cAMP was from Research Products (Mt. Prospect, IL); secondary antibody was from Antibodies Incorporated (Davis, CA); cAMP tracer was from New England Nuclear.

Tissue. Hormonally intact virgin female C57/Crl mice (≈16 g) were used at 5 weeks of age. BALB/c or C57 females were ovariectomized at 4 weeks of age to induce ductal regression and were used 3–6 months later.

Preparation of Implants. Implants were prepared by dispersing dry chemical in Elvax that had been dissolved in methylene chloride [20% (wt/vol)] and quick-freezing this mixture. After drying, the polymer matrix with entrapped chemical was cut to size (≈1 mg total weight) and implanted. The details of this procedure as well as the kinetics of release of various materials from Elvax have been described (15).

CT Dosage. Commercial CT contains 4.8% by weight of toxin protein, the bulk of the preparation being NaCl and Tris·HCl (55% and 37.6%, respectively). The most commonly used implant was prepared with 1 mg of the commercial preparation dissolved in 0.25 ml of Elvax. The dried Elvax pellet weighed ≈40 mg and contained 48 μg of toxin protein or 1.2 μg in an implant-sized piece weighing 1 mg. The useful dose range for this implant type is 0.1–1.2 μg of toxin.

Release of CT from Elvax. The release kinetics of CT was studied *in vitro*. Pellets prepared with either 1 mg or 10 mg of the toxin were cut into implant-sized pieces, weighed, and sealed in nylon bags (Nitex), which were then placed in 1.5 ml of normal saline at 37°C on a rotator (1 rpm). At 24-hr intervals, the bags were removed and the saline was assayed for protein against a CT standard using the Bradford method (16). Bags were then rinsed and replaced in fresh saline. An adequate amount of Elvax with toxin was available for three trials, one of which is shown here (Fig. 5); the release profile was the same for all three trials.

Surgical Implantation. The abdominal skin of Nembutal-anesthetized mice (60 μg/g of body weight) was cut and reflected to expose the underlying number 3 and 4 mammary glands. Iris scissors and Dumont forceps were used to place the implant. We have described the details of this surgery elsewhere (17).

Histology. Glands were fixed for 1–2 hr in either Tellyesniczky's or Carnoy's fixative. The protocol for hematoxylin staining of whole glands, as well as for alcian blue staining of paraffin sectioned material, has been described (17). Alcian blue staining in these experiments showed both nonsulfated (hyaluronate) and sulfated glycosaminoglycans.

DNA Autoradiography. For DNA autoradiography, animals were injected intraperitoneally with 100 μCi of [^{3}H]thymidine. After 30 min, the mammary gland was removed, fixed, and paraffin sectioned by standard methods. Slides were dipped in Kodak NTB-2 emulsion (diluted 1:1 with water), exposed for 10 days, and stained with hematoxylin/eosin after development.

Whole Gland DNA Synthesis. Thirty minutes prior to sacrifice, animals were injected with 100 μCi of [^{3}H]thymidine. To observe treatment effects against low background, isotope was injected at 1400 hr to coincide with the low point in

The publication costs of this article were defrayed in part by page charge payment. This article must therefore be hereby marked "*advertisement*" in accordance with 18 U.S.C. §1734 solely to indicate this fact.

Abbreviations: CT, cholera toxin; CT-A, CT subunit A; CT-B, CT subunit B.

mouse mammary gland DNA synthesis diurnal rhythm (18). Lymph nodes were removed and the glands were quick-frozen with dry ice, minced, and separated into two samples, each of which was weighed and homogenized. For one of the paired samples, total DNA was determined by fluorometry (19); DNA in the second sample was precipitated with cold 15% trichloroacetic acid (20), and the pellet was washed with cold ethanol/ether (3:1) and digested overnight in Protosol. Tritium radioactivity was determined by using standard procedures.

cAMP Determination. cAMP was determined by the radioimmunomethod of Steiner *et al.* (21). Tissue was quick-frozen between blocks of dry ice, weighed, minced, and homogenized in 1 ml of 6% ice-cold trichloroacetic acid. After centrifugation (Eppendorf Microfuge; 2 min) the supernatant was extracted three times with 3 ml of anhydrous ether and 0.1-ml aliquots were assayed after dilution (1:10) in reaction buffer.

RESULTS

Ovariectomy of virgin mice led within 4 weeks to end bud regression and a decrease in ductal diameter. Elvax implants containing CT stimulated end bud development and restored ductal caliber in regressed tissue (Fig. 1 *A* and *C*) while leaving contralateral (Fig. 1*D*) and ipsilateral glands (not pictured) unaffected. A gradient of stimulation (Fig. 1*C*) emphasizes the local effect of this treatment and indicates the diffusion of growth promotor from the implant. CT-A (the adenylate cyclase-activating subunit), implanted at a protein concentration approximately 5-fold greater than that found in a 1-mg implant of complete toxin, was not stimulatory (Fig. 1*B*) nor was the receptor-binding (CT-B) subunit (data not shown). The latter did, however, locally inhibit the effect of the complete toxin when both were implanted together (data not shown). Competitive inhibition of toxin action by CT-B has been reported for other systems (23). Elvax without additives (Fig. 1*D*) or with bovine serum albumin (data not shown) had no effect on regressed ducts.

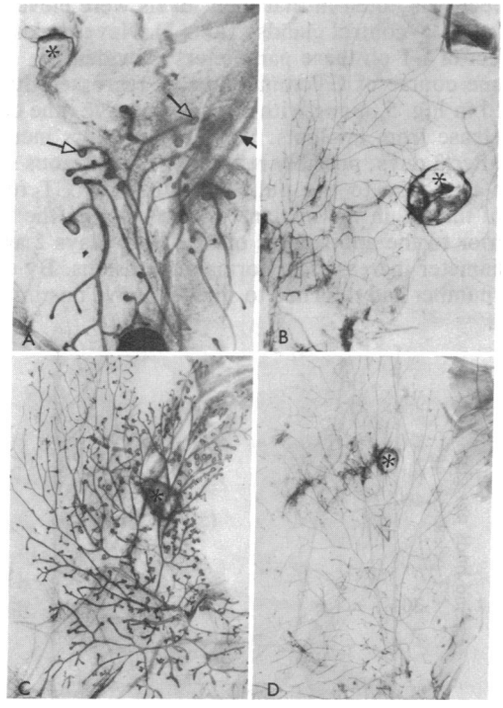

FIG. 1. Photomicrographs illustrating effects of CT and CT-A on ductal growth. (*A*) CT implant (0.34 μg; *) in the number 4 gland of an ovariectomized animal for 5 days stimulated end bud formation and restoration of ductal caliber. Open arrows point to end buds; the solid arrow points to a blood vessel; the large black object is a lymph node. (×3.85.) (*B*) CT-A implant (1.6 μg; *) in an ovariectomized animal for 5 days did not stimulate end bud formation. Since commercial CT-A preparations contain the same concentrations of NaCl and Tris·HCl as preparations of the complete toxin, the stimulatory effects of the complete toxin cannot be attributed to its nontoxin components. (×3.15.) (*C*) CT implant (0.47 μg; *) in the number 3 gland of an ovariectomized animal for 5 days stimulated extensive end bud formation. A gradient of stimulation is apparent both for end buds and for the diameter of subtending ducts. The diameter of ducts on the side of the gland opposite the implant approximates that seen in untreated control glands (*B* and *D*). (×2.7.) (*D*) Gland contralateral to that pictured in *C*. Implant (*) containing no additive was not stimulatory. Ducts lack end buds and are narrow in diameter, an appearance typical of glands in ovariectomized animals (22). (×2.7.)

Isoproterenol is a β-adrenergic receptor agonist that stimulates plasma membrane adenylate cyclase in a variety of cell types and has been shown to stimulate mammary epithelial cell division *in vitro* (1). Here it stimulated localized end bud development in ovariectomized animals (Fig. 2*A*), leaving other glands in the animal unaffected (data not shown). Both dibutyryl cAMP (Fig. 2*B*) and 8-bromo cAMP (data not shown) were implanted together with theophylline. These implants did stimulate end bud formation in ovariectomized animals; however, results were variable with neither the two cAMP derivatives nor isoproterenol proving as potent as CT. Forskolin, a diterpene activator of the catalytic element of receptor–adenylate cyclase complexes, was also stimulatory (data not shown) (24). Forskolin was more potent than dibutyryl cAMP, while butyrate alone had no effect. Stimulation often occurred at a distance of several millimeters from the implants (Figs. 1*A* and 2*A*), whereas some ducts directly adjacent to an implant sometimes remained unaffected (Fig. 2*B*). This may reflect a dose–response effect, differing epithelial sensitivity in different parts of the gland, or local peculiarities in blood and lymph circulation around implants or ducts.

Hormonally intact animals, whose glands already contained large end buds, responded to CT implants by developing small side branches on existing ducts that were not unlike the fine branching seen in early pregnancy (Fig. 3*A*). A gradient of stimulation was apparent, suggesting diffusion of growth promoter(s) from the implant. Also, several end buds

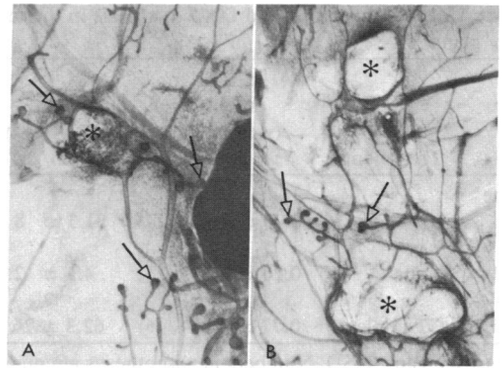

FIG. 2. Photomicrographs illustrating effects of isoproterenol and dibutyryl cAMP on regressed ducts. (*A*) Isoproterenol implant (170 μg; *) in an ovariectomized animal for 7 days stimulated end bud formation that was localized to the vicinity of the implant (open arrows). Ducts in distal parts of the implanted gland as well as in the nonimplanted contralateral and ipsilateral glands (data not shown) were unaffected. (×6.75.) (*B*) Dibutyryl cAMP (0.32 mg) combined with theophylline (0.14 mg) in each of two implants (*) in an ovariectomized animal for 6 days stimulated formation of several small end buds between the two implants (open arrows) while leaving ducts adjacent to the implants apparently unaffected. (×6.75.) Implants containing butyrate alone had no effect (data not shown).

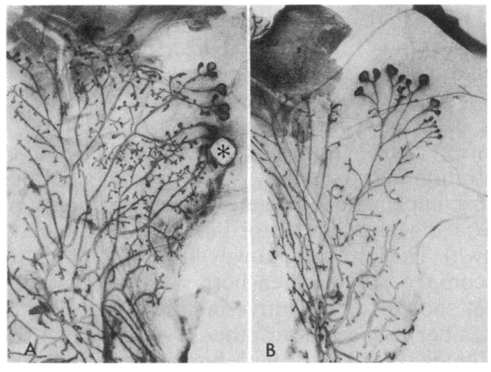

FIG. 3. Photomicrographs illustrating effects of CT on glands in hormonally intact 5-week-old animals. (*A*) CT implant (0.48 μg; *) in place for 5 days stimulated side branches on existing ducts. Stimulation was most intense near the implant, with end buds appearing to grow toward the CT source. (×4.05.) (*B*) Gland contralateral to that pictured in *A*. Note the absence of extensive side branching. (×4.05.)

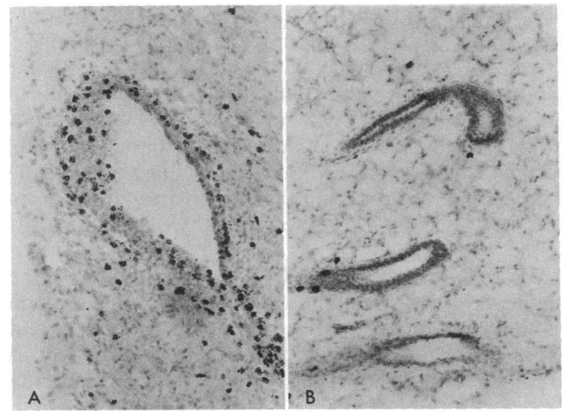

FIG. 4. DNA autoradiographs from untreated and CT-treated glands. (*A*) End bud in the vicinity of a CT implant in the gland pictured in Fig. 1*A*. Extensive labeling is seen in the epithelium, with some labeling also visible in the stroma. (×180.) (*B*) Gland contralateral to that pictured in *A*. The lack of epithelial labeling and the small size of the regressed ducts are apparent. (×180.)

appear to have grown toward the implant, suggesting tropism. The contralateral glands were unaffected by the implant as evidenced by the open ductal spacing relatively free of side branches (Fig. 3*B*).

cAMP levels in glands from ovariectomized animals were lower than those in hormonally intact animals by a factor of almost 4. At CT doses that stimulated regressed ducts to form end buds, cAMP was elevated to levels comparable with those of hormonally intact animals (Table 1). These levels were similar to those obtained by others using glands from virgin animals (9).

DNA synthesis in mammary glands of ovariectomized mice was also significantly lower than levels found in endocrine-intact animals (by a factor of 7) (Table 1). CT-treated glands from ovariectomized animals showed a sharp increase in DNA synthesis over the contralateral controls, as shown autoradiographically (Fig. 4) and by whole gland measurements (Table 1). DNA synthesis in stromal cells surrounding the epithelial end buds was also increased (Fig. 4*A*), resembling that associated with vigorously growing normal glands (25). With both DNA synthesis and cAMP, a systemic effect was noted in that their levels were elevated in the contralateral control glands (Table 1). Nevertheless, the local effect of CT on these parameters is evident.

The time course of CT stimulation of regressed ducts is illustrated in Fig. 5, along with a representative time course of CT release from implants. End bud numbers increased sharply after 3 days, possibly reflecting synchronous stimulation in response to the pulsatile nature of CT release (≈30% of the CT in the implant was released in the first 2 days). Prior to the appearance of end buds (days 2 and 3), ductal diameter increased to normal dimensions. By day 6, end bud number had returned to slightly above unstimulated

Table 1. cAMP concentration and DNA synthesis in the mouse mammary gland

Animal	Treatment	cAMP, pmol/mg (wet weight) tissue	DNA synthesis, cpm/μg DNA
Endocrine intact	None	0.76 ± 0.2 (23)	31.3 ± 8 (10)
Ovariectomized	None	0.20 ± 0.06 (13)	4.3 ± 2.5 (12)
Ovariectomized	CT implant	0.77 ± 0.27* (6)	62.3 ± 26 (8)†

Results are means ± SD. Numbers in parentheses are numbers of glands assayed.

*Implants contained 0.34–0.53 μg of CT and were in place for 4 days before sacrifice. As glands were removed they were examined for end buds. In the animal with the lowest dose (0.36 μg of CT in two glands), no end buds were seen in the nonimplanted contralateral gland, which had a cAMP level of 0.34 pmol/mg (wet weight) of tissue. In the two animals receiving a higher dose (0.48 μg of CT in two glands), end buds were observed contralaterally and values for cAMP of 0.55 and 0.73 pmol/mg (wet weight) of tissue were obtained.

†Implants contained 0.86 μg of CT and were in place 5 days prior to sacrifice. At this dose, DNA synthesis in the nonimplanted contralateral gland was 26.2 ± 10.6 cpm/μg of DNA.

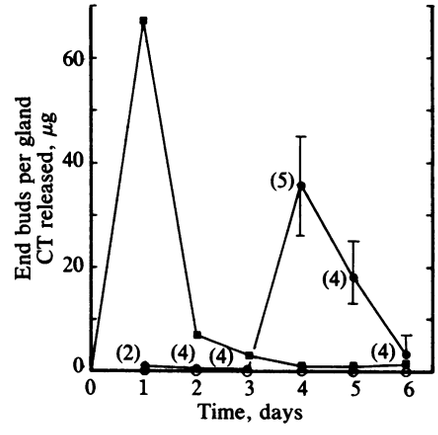

FIG. 5. Time course of CT-stimulated end bud formation and CT release. Ovariectomized animals implanted with 0.8 μg of CT (●) and with blank implants in the contralateral glands (○) were sacrificed on the indicated days, whole glands were removed and stained, and numbers of end buds were counted. Each point represents mean ± 95% confidence interval. Results are from two experiments; numbers of glands examined for each time point are shown in parentheses. A representative plot (■) of *in vitro* CT release is shown for the implant used in this study. The initial amount of CT was 276 μg; this was distributed in several dozen implant-sized pieces of Elvax. The percentage recovery after 6 days was 30; after the first 3 days, release was ≈1 μg/day. An initial rapid release of incorporated material is characteristic of Elvax implants (15), while subsequent slow release may occur when the starting amount in the matrix is low (<1 mg) (26). Implants containing amounts of CT different from that used in this experiment had release profiles identical to the one pictured here.

levels. One or two end buds were still present after 12 days, and complete regression followed. Sequential implantation of CT into the same gland (one implant per week for 3 weeks) produced severe inflammation and prolonged gland growth was not obtained.

The architecture of CT-treated glands from ovariectomized animals was compared with that of glands from untreated 5-week-old hormonally intact animals. End buds induced by CT appeared smaller than normal. Also, their shape was somewhat more variable than normal, while subtending ducts were of normal size and generally lacked unusual outgrowths (compare Fig. 1 *A* and *C* with Fig. 3*B*). The cellular architecture of toxin-induced end buds was not distinguishable from that of end buds in untreated animals (Fig. 6). Importantly, the cap cells, a stem cell layer that overlies the tip of normal end buds, was present with a characteristic space between it and the body of the end bud (13). Alcian blue, a stain that is specific for glycosaminoglycans, was used to visualize the basal lamina and the epithelial–stromal interface (Fig. 6). The basal lamina stained faintly in the cap region and somewhat more intensely on the immediately subtending duct, a pattern seen in normal end buds (27). The generally lower staining intensity in toxin-induced end buds suggests that they may differ from normal with respect to basal lamina glycosaminoglycans.

Stromal arrangement around the CT-induced end buds appeared normal (Fig. 6). As in 5-week-old tissue, adipocytes were closely apposed to the cap cells, while differentiation of fibrous elements (which become the collagenous tunic of the duct) was first evident on the flank of the end bud just below its point of maximum diameter.

The response of regressed mammary ducts to CT over a 100-fold dose range is shown in Fig. 7. The response of the regressed gland to different concentrations of CT ranged from slight ductal distention and enlargement of regressed tips at low concentrations to occasional intense stimulation where end buds crowd into normally open interductal space. Over the complete dose range, the gland responded only with end bud growth and side branching; in no case was alveolar stimulation seen. Also, in >130 CT implant experiments, the only abnormality that we observed was a small ductal hyperplasia lying directly against an implant.

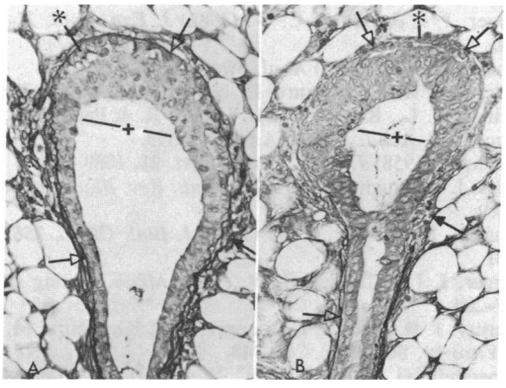

FIG. 6. Photomicrographs of end bud sections from a 5-week-old untreated animal and a CT-implanted (0.4 μg; 5 days) ovariectomized animal. Tissue was stained with alcian blue to show both sulfated and nonsulfated glycosaminoglycans (0.1% stain; 0.3 M $MgCl_2$, pH 5.8; 45 min). (*A*) In the untreated animal the basal lamina (open arrows) stained most intensely on the end bud flanks. Stromal differentiation began near the point of maximum diameter (+) of the end bud and was characterized by lines of alcianophilic material interspersed with collagen fibers (solid arrow). Large, extracellular spaces separated the cap cell layer (*) from the underlying epithelium. (×180.) (*B*) CT-induced cellular architecture of the end bud was similar to those in untreated glands, with cap cells (*) apparent and stromal differentiation adjacent to the flank beginning at the point of maximum diameter (+) of the end bud. Alcian blue staining in the basal lamina (open arrows) and adjacent stroma (solid arrow) appeared less intense. (×180.)

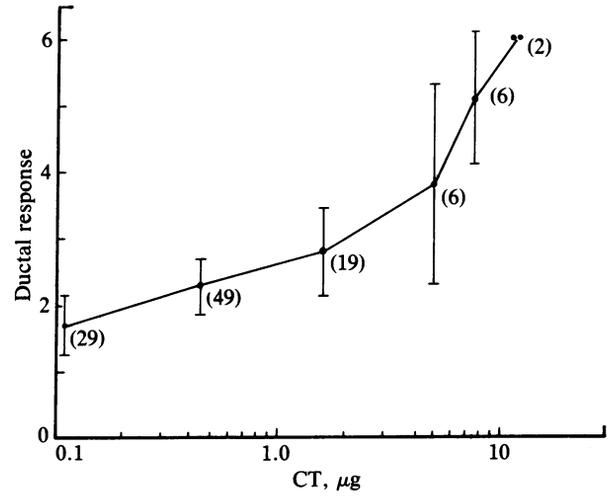

FIG. 7. CT dose–response in ovariectomized animals. Most animals received a single implant in the right number 4 gland with the ipsilateral and contralateral glands counted as controls. In some animals both the right number 3 and 4 glands were implanted. Glands with <5% of the fat pad containing ducts, indicating poor growth prior to ovariectomy and treatment, were not counted. Of the total glands treated (124, all doses), 90% responded positively. Some stimulation of control glands occurred in 12% (17) of the 140 untreated glands. Numbers of glands treated are shown in parentheses; error bars represent 95% confidence intervals. The following criteria were used to score glands: 0, ductal tips are same diameter as subtending ducts, which are spindly; +1, some but not all duct tips are enlarged, no end buds, ductal diameter is unaffected; +2, small end buds are present, enlarged tips, ductal diameter is increased; +3, larger end buds are present but they are few in number (<10), ductal diameter is increased; +4, numerous end buds (10–20) are present but some tips remain unstimulated, ductal diameter is comparable with that of hormonally intact animal; +5, entire gland appears stimulated, many end buds (>20) are present; +6, as in +5 but the gland is intensely stimulated in places with "grape cluster" outgrowths on some ducts.

DISCUSSION

In experiments conceptually analogous to classical endocrine ablation/replacement studies, we have demonstrated that mouse mammary duct regression due to ovariectomy can be locally reversed by cAMP-active agents (Figs. 1 *A* and *C* and 2). In this case, stimulation was achieved by elevating the level of an intracellular effector of hormone or growth factor action, rather than by replacing the extracellular mitogen itself (Table 1).

The inactivity of CT-A (Fig. 1*B*) and CT-B, as well as of bovine serum albumin (not shown) showed that stimulation was not due to nonspecific effects of foreign protein. On the contrary, specificity for cAMP was shown by the efficacy of cAMP derivatives as well as that of agents known to activate separate elements of the adenylate cyclase system [isoproterenol stimulates cell surface β-adrenergic receptors; CT irreversibly activates the guanine nucleotide-binding regulatory unit (28); forskolin reversibly activates the catalytic element of this system (24)]. CT was considerably more potent than isoproterenol or dibutyryl cAMP, an observation supported by similar results with mouse mammary epithelia *in vitro* (1) and consistent with its irreversible effect on the cyclase.

The question of where cAMP has its primary effect, on epithelia or stroma, is not answered by these experiments

but, based on the growth-stimulating effects of cAMP-agents on pure cultures of mammary epithelia, it is most likely that our results are due in part to increased levels of cAMP in mammary epithelial cells. On the other hand, end bud formation and normal ductal growth are not achieved in culture, and the importance of stroma in directing mammary morphogenesis has been documented (29). Since CT implants no doubt raise cAMP levels in stroma as well as in epithelial areas, a stromal component to the observed effect is quite plausible.

Based on several criteria, the growth stimulated by cAMP in either regressed or growing glands was apparently normal. Whole gland growth patterning is considered to be a sensitive indicator of mammary morphogenetic and cellular regulation; abnormalities such as dysplasias and hyperplasias can be readily seen (30) and were notably absent in treated glands. cAMP stimulation produced end buds that were similar in shape but generally smaller in size (Figs. 1 *A* and *C* and 2) compared with those in untreated growing glands (Fig. 3*A*). Ductal dimensions were also similar to those seen in untreated growing glands. One unusual aspect of CT stimulation was the crowding of end buds into normally open interductal spaces (Fig. 1*C*), suggesting that cAMP stimulation overcame restrictions on ductal growth into space occupied during pregnancy by secretory epithelium. While the absence of lobulo-alveolar differentiation indicates that cAMP stimulated a specific ductal-morphogenetic pathway, it remains to be seen whether the fine branching stimulated by CT in hormonally intact animals (Fig. 3*A*) becomes alveolar on extended treatment.

The absence of abnormal patterns of gland growth over a 100-fold CT dose range (Fig. 7) and the reversibility of stimulation (Fig. 5), as well as the infrequent appearance of hyperplastic or dysplastic growth observed in mammary tissue treated with CT *in vitro* (31), also support the argument that cAMP is operating through a normal morphogenetic pathway.

The detailed cellular architecture and stromal association of CT-induced end buds were indistinguishable from untreated counterparts (Fig. 6). Two points are of particular interest: first, restoration of the ductal stem cell layer (cap cells) strongly indicates that cAMP stimulates a normal morphogenetic pathway since these cells are putative receptors for growth regulatory signals and as such are considered to be responsible for normal structural development (13). Second, given the demonstrated influence of the stroma on the form and growth of mammary epithelium, it is significant that cAMP restored typical epithelial-stromal associations including stromal DNA synthesis (Fig. 4), as this suggests that cAMP, directly or indirectly, restored and maintained the normal morphogenetic reciprocity between the two tissues.

In a variety of developing tissues, including the mouse mammary gland, glycosaminoglycans are associated with morphogenesis and may influence growth regulation (27, 32). Decreased alcian blue staining of basal lamina and adjacent stroma around CT-induced end buds is potentially important (Fig. 6), as it suggests that hyaluronate, a glycosaminoglycan associated with rapidly growing tissue and known to stain lightly with alcian blue, may predominate in the extracellular region of this tissue. Although cause and effect are obscure with respect to the role of glycosaminoglycans in development, hyaluronate is considered to be permissive, if not stimulatory, to cell proliferation and movement (32). cAMP is known to influence glycosaminoglycan synthesis (33, 34), stimulating hyaluronate production in rat fibroblasts *in vitro* (35). It is possible, therefore, that cAMP may be influencing ductal growth and morphogenesis through modulation of specific glycosaminoglycans.

The tight coupling of mitosis and morphogenesis that was maintained under cAMP stimulation must require the coordinated regulation of numerous complex functions, including mitosis, basement membrane synthesis (27), establishment of membrane junctions (13), and possibly the elaboration of secondary extracellular signals to coordinate epithelial and stromal interactions. Although our results show that cAMP can orchestrate these functions, it remains to be seen whether cAMP is the natural mediator of ductal mammogenic signals. Alternatively, cAMP-stimulated protein kinase activity may partially overlap that of protein kinases activated by growth regulators such as epidermal growth factor.

We thank Linda Wilson for technical assistance. This work was supported by National Science Foundation Grant PCM-8308145 and National Institute on Aging Grant AG 01050.

1. Yang, J., Guzman, R., Richards, J., Imagawa, W., McCormick, K. & Nandi, S. (1980) *Endocrinology* **107,** 35–41.
2. Pasco, D., Quan, A., Smith, S. & Nandi, S. (1982) *Exp. Cell Res.* **141,** 313–324.
3. Stampfer, M. R. (1982) *In Vitro* **18,** 531–537.
4. Taylor-Papadimitriou, J., Purkis, P. & Fentiman, I. S. (1980) *J. Cell. Physiol.* **102,** 317–321.
5. Green, H. (1978) *Cell* **16,** 801–816.
6. Marcelo, C. L. & Duell, E. A. (1978) *J. Invest. Dermatol.* **70,** 211 (abstr.).
7. Guidotti, A., Weiss, B. & Costa, E. (1972) *Mol. Pharmacol.* **8,** 521–530.
8. Armato, U., Draghi, E. & Andreis, P. G. (1977) *Exp. Cell Res.* **105,** 337–347.
9. Rillema, J. A. (1976) *Proc. Soc. Exp. Biol. Med.* **151,** 748–751.
10. Sapag-Hagar, M. & Greenbaum, A. L. (1974) *FEBS Lett.* **46,** 180–183.
11. Minton, S. P., Mathews, R. H. & Wisenbaugh, T. W. (1976) *J. Natl. Cancer Inst.* **57,** 39–41.
12. Kung, W., Bechtel, E. & Geyer, E. (1977) *FEBS Lett.* **82,** 102–105.
13. Williams, J. M. & Daniel, C. W. (1982) *Dev. Biol.* **97,** 274–290.
14. Bresciani, F. (1968) *Cell Tissue Kinet.* **1,** 51–63.
15. Rhine, W. D., Hsieh, D. S. T. & Langer, R. L. (1980) *J. Pharmacol. Sci.* **69,** Suppl. 3, 265–270.
16. Bradford, M. (1976) *Anal. Biochem.* **72,** 248–254.
17. Silberstein, G. B. & Daniel, C. W. (1982) *Dev. Biol.* **93,** 272–278.
18. Berger, J. J. & Daniel, C. W. (1982) *J. Exp. Zool.* **224,** 115–118.
19. Hinegardner, R. (1971) *Anal. Biochem.* **39,** 197–201.
20. Hutchison, W. C. & Munro, H. N. (1961) *Analyst* **86,** 768–813.
21. Steiner, A. L., Kipnis, D. M., Utiger, R. & Parker, C. (1969) *Proc. Natl. Acad. Sci. USA* **64,** 367–373.
22. Nandi, S. (1958) *J. Natl. Cancer Inst.* **21,** 1039–1055.
23. Moss, J. & Vaughan, M. (1979) *Annu. Rev. Biochem.* **48,** 581–600.
24. Seamon, K. & Daly, J. W. (1981) *J. Biol. Chem.* **256,** 9799–9801.
25. Berger, J. J. & Daniel, C. W. (1983) *Mech. Ageing Dev.* **23,** 277–284.
26. Murray, J. B., Brown, L., Langer, R. & Klagsburn, M. (1983) *In Vitro* **19,** Suppl. 10, 743–748.
27. Silberstein, G. B. & Daniel, C. W. (1982) *Dev. Biol.* **90,** 215–222.
28. Nielsen, T. B., Lad, P. M., Preston, S. & Rodbell, M. (1980) *Biochim. Biophys. Acta* **629,** 143–155.
29. Sakakura, T., Nishizuka, Y. & Dawe, C. J. (1976) *Science* **194,** 1439–1441.
30. Ethier, S. P. & Ullrich, R. L. (1982) *Cancer Res.* **42,** 1753–1760.
31. Schaefer, F. V., Custer, R. P. & Sorof, S. (1980) *Nature (London)* **286,** 807–810.
32. Toole, B. P. (1981) in *Cell Biology of the Extracellular Matrix,* ed. Hay, E. D. (Plenum, New York), pp. 259–288.
33. Greene, R. M., MacAndrew, V. I. & Lloyd, M. (1982) *Biochem. Biophys. Res. Commun.* **107,** Suppl. 1, 232–238.
34. Stack, M. T. & Brandt, K. D. (1980) *Biochim. Biophys. Acta* **631,** 264–277.
35. Tomida, M., Koyama, H. & Ono, T. (1977) *Biochem. J.* **162,** 539–543.